

Long-horizon model predictive control of induction motor drive

KAROL TOMASZ WRÓBEL, KRZYSZTOF SZABAT, PIOTR SERKIES

*Department of Electrical Machines, Drives and Measurements
Wroclaw University of Science and Technology
Smoluchowskiego 19, 50-372 Wroclaw, Poland
e-mail: {karol.wrobel/krzysztof.szabat/piotr.serkies}@pwr.edu.pl*

(Received: 19.11.2018, revised: 03.04.2019)

Abstract: This paper investigates the application of a novel Model Predictive Control structure for the drive system with an induction motor. The proposed controller has a cascade-free structure that consists of a vector of electromagnetics (torque, flux) and mechanical (speed) states of the system. The long-horizon version of the MPC is investigated in the paper. In order to reduce the computational complexity of the algorithm, an explicit version is applied. The influence of different factors (length of the control and predictive horizon, values of weights) on the performance of the drive system is investigated. The effectiveness of the proposed approach is validated by some experimental tests.

Key words: model predictive control, long horizon, induction motor drive

1. Introduction

Advances in microprocessor techniques visible over the last decades have led to a huge rise of computational power. This allows for the implementation of many sophisticated control methodologies in cases, where computational complexity is their main limitation. In addition, progress in power electronics allows one to obtain reliable and flexible supply sources. These two factors, combined with industrial demand for high-performance motion systems, justify the development of new control structures for electrical drives [1–11].

There are many approaches to the design of the control structure for a modern drive system. Usually, this process is divided into two main points. Based on the cascade concepts the torque control loop is designed first. Then the controller for speed/position control is considered. In almost all evident approaches these two problems are considered and solved separately. In order



to regulate the electromagnetic torque, different control strategies have been developed depending on the types of machine used (DC/AC) and requirements. One of the most popular methods for AC motor control is direct field oriented control (DFOC) structure. It has a relatively complicated algorithm, in which four controllers (including a speed problem) and transformation blocks are visible. The mentioned controllers are tuned separately for the assumed linear operation point. However, the changes of working conditions worsen the drive performances.

Over the last few decades the MPC has gained a lot of attention from the control engineering community. It is due to the fact that the computational power of a microprocessor is strong and is still growing, nowadays. Therefore, the research of the advanced control algorithms is justified and expected. Generally, the MPC uses a model of the plants to predict the future values of the system states. The optimal control sequence is selected on the basis of the cost function solving the optimization problem. Different groups of the MPC are described in the literature. The first classification depends on the character of the control signal and the MPC can be divided into continuous set (CS) and finite-set (FS) algorithms. In the CS-MPC, the control signal can take all values within some range, while in the FS-MPC it is limited to some values. The next classification depends on the algorithm implementation form and it produces two main groups. In the first one the optimization problem is solved on-line, which means that the computational complexity of this approach is high. The second group possesses an algorithm in which the optimization problem is computed off-line and which is generally called explicit-MPC. The other classification depends on the length of the prediction horizon: so short- and long-horizon MPC is considered.

The literature provides a number of papers describing different applications of the MPC in the area of power electronics and electrical drives. Usually, the FS short-horizon MPC is applied in order to control power converters. It comes from the discrete nature of the power electronic elements, in which only two main states can be recognized: on or off. This approach can also be easily implemented for non-linear systems. The drawback of such a system is the relatively high computational complexity of the nonlinear MPC, so usually the length of the prediction horizon is set to one or two samples ahead.

In the case of motion control, the situation is different. It results from the following reasons: a modern electrical drive consists of a power converter, electromagnetic and mechanical parts of the motor. The time constants connected with electromagnetic parameters are much shorter than those connected with mechanical ones, which causes high computational requirements for one common controller. One of the ways of decreasing the computational complexity is to apply multisampling strategies, separately for electromagnetic and mechanical parameters. However, due to the continuous increase of microprocessor computational power, the design and real-time application of one common controller is possible.

The most natural approach to the MPC is based on the complete nonlinear model of an electrical motor and discrete nature of a power converter. This framework is presented in [12–14], where the application of FS-MPC for a permanent magnet synchronous motor (PMSM) is demonstrated. The four classical PI controllers are eliminated and the switches of the power converter are directly controlled by an algorithm. However, due to computational complexity the only one-step horizon is used. This limits the effectiveness of the classical MPC strategy, where the length of horizon plays a crucial role in the algorithm, especially for the nonlinear plant with constraints. The explicit version of the generalized predictive control of a PMSM is presented in [15]. In order to decrease the computational complexity, the linear model of a plant is employed. In [16] the

cascade-free speed MPC for an induction motor (IM) drive is proposed. The predictive algorithm controls the flux and the speed of the motor simultaneously, offering a good performance of the drive. The explicit version of the MPC is used. In order to decrease further computational complexity of the system, different tree-searching strategies are analyzed.

The main point of the work is to present the design methodology and performance analysis of the MPC-based control structure for a drive system with an IM. Similarly to modern approaches evident in the literature [17, 18] there is no division into the torque and speed control loops. The rotor flux and speed of the system are controlled by one predictive algorithm. Although the long-horizon MPC is a traditional approach, there are limited works presenting its application in the area of an electrical drive and power electronics, where usually FS-MPC with a short horizon (one or two steps ahead) is used. In order to reduce the drawback of the traditional MPC, which is characterized by high computational complexity, two solutions are applied. Firstly, the model of an IM is linearized by decoupling circuits. Secondly, the explicit version of an MPC controller is used. Different control factors as length of the control and predictive horizon, weights in the cost function are analyzed. The performance of the system are tested under variety of simulation tests. Also some experimental tests are included.

2. Model predictive control

In model predictive control, an explicit model of a plant is used to predict the effect of future actions of the manipulated variables on the process output [19]. In the recent literature, the following linear discrete-time state-space model is typically employed

$$\begin{aligned} \mathbf{x}(k+1) &= \mathbf{A}\mathbf{x}(k) + \mathbf{B}\mathbf{u}(k), \\ \mathbf{y}(k) &= \mathbf{C}\mathbf{x}(k), \end{aligned} \quad (1)$$

where $\mathbf{x}(t) \in \mathfrak{R}^n$, $\mathbf{u}(t) \in \mathfrak{R}^m$, $\mathbf{y}(t) \in \mathfrak{R}^p$ denote the system state, input and output vectors, respectively. $\mathbf{A} \in \mathfrak{R}^{n \times n}$, $\mathbf{B} \in \mathfrak{R}^{n \times m}$, $\mathbf{C} \in \mathfrak{R}^{p \times n}$ are the matrices describing the dynamics of the plant, k is the discrete time constant.

At each time step k , the MPC algorithm solves the following optimization problem [19]:

$$\min_{\mathbf{u}_0^T, \dots, \mathbf{u}_{N_c-1}^T} \left\{ \sum_{i=0}^N (\mathbf{y}_{k+i|k}^{\text{ref}} - \mathbf{y}_{k+i|k})^T \mathbf{Q} (\mathbf{y}_{k+i|k}^{\text{ref}} - \mathbf{y}_{k+i|k}) + \sum_{i=0}^{N_u-1} \mathbf{u}_{k+i|k}^T \mathbf{R} \mathbf{u}_{k+i|k} \right\}, \quad (2a)$$

$$\begin{aligned} \mathbf{u}_{\min} \leq \mathbf{u}_{k+i|k} \leq \mathbf{u}_{\max}, \quad i = 0, 1, \dots, N_u-1; \quad \mathbf{y}_{\min} \leq \mathbf{y}_{k+i|k} \leq \mathbf{y}_{\max}, \quad i = 0, 1, \dots, N, \\ \mathbf{x}_{k+i+1|k} = \mathbf{A}\mathbf{x}_{k+i|k} + \mathbf{B}\mathbf{u}_{k+i}, \quad i \geq 0, \quad \mathbf{y}_{k+i|k} = \mathbf{C}\mathbf{x}_{k+i|k}, \quad i \geq 0, \quad \mathbf{x}_{k|k} = \mathbf{x}(k), \end{aligned} \quad (2b)$$

where $\mathbf{Q} \geq 0$ and $\mathbf{R} > 0$ are the weighting matrices, N and N_u denote the prediction and control horizon, respectively, and \mathbf{u}_{\min} , \mathbf{u}_{\max} , \mathbf{y}_{\min} , and \mathbf{y}_{\max} are the input and output constraints of the system. The following inequality is held in the system $N_u \leq N$.

Equation (2a) can be written in the form of a matrix using quadratic programming (QP) [20]:

$$J(\mathbf{U}, \mathbf{x}(k)) = \mathbf{X}^T \tilde{\mathbf{Q}} \mathbf{X} + \mathbf{U}^T \tilde{\mathbf{R}} \mathbf{U}, \quad (3)$$

where $X \in \mathfrak{R}^N$ and $U \in \mathfrak{R}^{N_u}$ are the predictive vectors of state variables and controls:

$$X(k) = \begin{bmatrix} x(k + N_1|k) \\ \vdots \\ x(k + N|k) \end{bmatrix}, \quad U(k) = \begin{bmatrix} u(k|k) \\ \vdots \\ u(k + N_u - 1|k) \end{bmatrix}. \quad (4)$$

The matrices $\tilde{Q} \in \mathfrak{R}^{N \times N}$ and $\tilde{R} \in \mathfrak{R}^{N_u \times N_u}$ have the following form:

$$\tilde{Q} = \begin{bmatrix} Q & 0 & 0 \\ 0 & \ddots & 0 \\ 0 & 0 & Q \end{bmatrix}, \quad \tilde{R} = \begin{bmatrix} R & 0 & 0 \\ 0 & \ddots & 0 \\ 0 & 0 & R \end{bmatrix}. \quad (5)$$

Finally, the problem of optimal control using quadratic programming can be formulated as:

$$V(x(k)) = x(k)^T Y x(k) + \min_U \left(\frac{1}{2} U^T H U + x'(k)^T F U \right), \quad (6)$$

subject to $GU \leq W + Ex(k)$,

where: H, F, Y are defined as follows:

$$H = \tilde{B}^T \tilde{Q} \tilde{B} + \tilde{R}, \quad F = \tilde{A}^T \tilde{Q} \tilde{B}, \quad Y = \tilde{A}^T \tilde{Q} \tilde{A}, \quad (7)$$

$$\tilde{A} = \begin{bmatrix} I \\ A \\ \vdots \\ A^{N_u} \\ \vdots \\ A^N \end{bmatrix}, \quad \tilde{B} = \begin{bmatrix} 0 & \cdots & 0 \\ B & \cdots & 0 \\ \vdots & \ddots & \vdots \\ A^{N_u} & \cdots & B \\ \vdots & \vdots & \vdots \\ A^{N-1} x B & \cdots & \sum_{i=0}^{N-N_u} A^i B \end{bmatrix}. \quad (8)$$

The MPC algorithm based on problem (2) can be implemented in two ways. Traditionally, the optimization problem is solved *on-line* for a given $x(k)$ in a receding-horizon fashion. So, at a given time k , only the first element of the control signal u_k is implemented to the system and the rest of the control sequence is discarded. Then, the whole procedure is repeated in the next step ($k + 1$) for the new output $y(k + 1)$ [21–23]. This strategy is computationally demanding for systems with fast-changeable variables and requires high-performance processors. In the second approach, problem (2) is solved *off-line* for all possible state realizations within some compact set X_f using multi-parametric programming [24–26]. Specifically, by treating the state vector $x(k)$ as a parameter vector, it can be shown that the parameter space X_f can be subdivided into characteristic regions, where the optimizer is given as an explicit function of the parameters. This profile is a piecewise affine state feedback law:

$$U(x) = K_r x + g_r, \quad \forall x \in P_r, \quad (9)$$

where P_r represents the polyhedral sets defined as:

$$P_r = \{x \in \mathfrak{R}^n | H_r x \leq d_r\}, \quad r = 1, \dots, N_r \quad (10)$$

and N_r denotes the total number of polyhedral regions in the partition [25–27].

3. Mathematical model of the plant and MPC structure

In the study, the mathematical model of the induction motor using the space vector with orientation on the rotor flux in per unit system is presented. The IM is described by the following equations taking into account the commonly-used simplification [28].

$$T_N \frac{d\Psi_r}{dt} = \frac{r_r x_M}{x_r} i_{sx} - \frac{r_r}{x_r} \Psi_r, \quad (11)$$

$$0 = \frac{r_r x_M}{x_r} i_{sy} - \omega_r \Psi_r, \quad (12)$$

$$m_e = \frac{x_M}{x_r} (\Psi_r i_{sy}). \quad (13)$$

The motion equations are formulated as:

$$\frac{d}{dt} \omega = \frac{1}{T_l} (m_e - m_L), \quad (14)$$

where \mathbf{u}_s is the vector of the stator voltage, $\mathbf{i}_s, \mathbf{i}_r$ are the vectors of the stator and rotor currents, Ψ_s, Ψ_r are the vectors of the stator and rotor flux, ω_r is the slip pulsation, T_N is the reference time constant, r_s, r_r represent the stator and rotor resistance, x_s, x_r, x_M represent the reactance of the stator, rotor and magnetising, T_M is the mechanical time constant.

In order to decouple the flux and torque control loops, the additional components are calculated and inserted to systems (15)–(20) [28]:

$$\mathbf{u}_{sk} = r_s \mathbf{i}_{sk} + T_N \frac{d}{dt} \Psi_{sk} + j\omega_k \Psi_{sk}, \quad (15)$$

$$\Psi_{sk} = x_s \mathbf{i}_{sk} + x_M \mathbf{i}_{rk}, \quad (16)$$

$$\Psi_{rk} = x_r \mathbf{i}_{rk} + x_M \mathbf{i}_{sk}, \quad (17)$$

$$\mathbf{u}_s = r_s \mathbf{i}_s + T_N x_s \sigma \frac{d\mathbf{i}_s}{dt} + j\omega_{s\psi} x_s \sigma \mathbf{i}_s + \frac{x_M}{x_r} T_N \frac{d\Psi_r}{dt} + j\omega_{s\psi} \frac{x_M}{x_r} \Psi_r, \quad (18)$$

$$u_{sx} = r_s i_{sx} + T_N x_s \sigma \frac{di_{sx}}{dt} - \underbrace{\omega_{s\psi} x_s \sigma i_{sy} + \frac{x_M}{x_r} T_N \frac{d\Psi_r}{dt}}_{e_x}, \quad (19)$$

$$u_{sy} = r_s i_{sy} + T_N x_s \sigma \frac{di_{sy}}{dt} + \underbrace{\omega_{s\psi} x_s \sigma i_{sx} + \omega_{s\psi} \frac{x_M}{x_r} \Psi_r}_{e_y}, \quad (20)$$

where σ is the total engine scattering factor, $\omega_{s\psi}$ is the field pulsation, $\mathbf{u}_{sk}, \mathbf{i}_{sk}, \Psi_{sk}$ are the vectors of the stator voltage, current and flux rotating with the speed ω_k , in this case $\omega_k = \omega_{s\psi}$.

The decoupling algorithm allows one to transform the model of an IM from a time-varying to time-invariant system.

The considered control structure is presented in Fig. 1. It consists of one MPC controller which replaces four controllers evident in DFOC. On the basis of the system states, the MPC

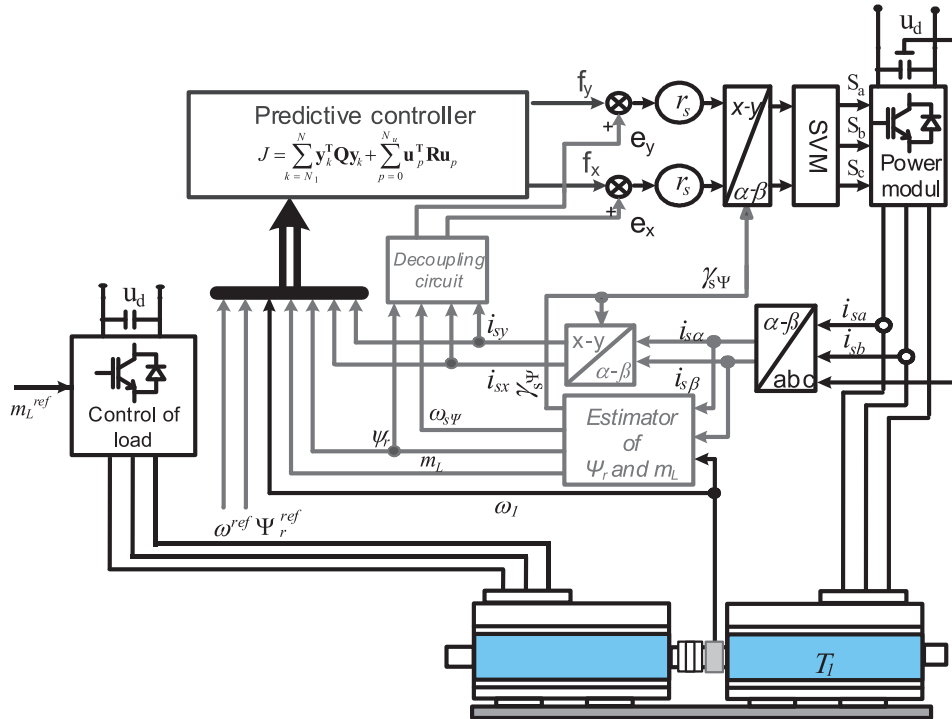


Fig. 1. The MPC-based control structure

generates two control signals for speed and torque paths. The switching frequency in this structure is constant and determined by the sampling frequency of the modulator (10 kHz).

The traditional control structure (DFOC) relies on the classical cascade concept and therefore possesses its features. It can be applied to the system whose inner (torque) loop is much faster than outer (speed) loops, which is usually fulfilled in an electrical drive. In this structure the tuning methodology is quite simple (each controller is adjusted separately) and the limitation of the inner one can be set as a constant value. As its drawbacks, the relatively slow reaction to the changes of disturbances or reference values can be enumerated. The MPC controller has a similar structure to the state-controller: there are no inner separate loops in the scheme, which increases the dynamics of the system against the changes of the reference signal and the disturbances. Also, the simultaneous control of two variables (speed, flux) can, in some cases, be treated as an advantage. An additional feature of the MPC structure is a possibility of introduction of soft constraints (contrary to hard constraints evident in the classical system). Also, a big advantage is ability to formulate a cost function in such a way that not only the dynamics but also the cost of energy is included. All those factors allow one to generate an optimal control signal of the MPC. However, there are also drawbacks: more complicated algorithms and the necessity of experience in formulating a cost function.

The discrete model of the plant in the MPC is built based on electromagnetic (11)–(13) and motion (15) equations. The decoupling terms of (19), (20) allow one to treat the system as linear

and apply an explicit MPC algorithm. The state vector is extended by two reference variables for rotor flux and speed. The matrices of the system are presented below (21):

$$A = \begin{bmatrix} \frac{-r_s}{\sigma T_N x_s} & 0 & 0 & 0 & 0 & 0 & 0 \\ \frac{x_M r_r}{x_r T_N} & \frac{-r_r}{x_r T_N} & 0 & 0 & 0 & 0 & 0 \\ 0 & 0 & \frac{-r_s}{\sigma T_N x_s} & 0 & 0 & 0 & 0 \\ 0 & 0 & \frac{\psi_r^{nom} x_M}{x_r T_1} & 0 & \frac{1}{T_1} & 0 & 0 \\ 0 & 0 & 0 & 0 & 0 & 0 & 0 \\ 0 & 0 & 0 & 0 & 0 & 0 & 0 \\ 0 & 0 & 0 & 0 & 0 & 0 & 0 \end{bmatrix}, \quad B = \begin{bmatrix} \frac{1}{\sigma T_N x_s} & 0 \\ 0 & 0 \\ 0 & \frac{1}{\sigma T_N x_s} \\ 0 & 0 \\ 0 & 0 \\ 0 & 0 \\ 0 & 0 \end{bmatrix}, \quad (21)$$

$$u = \begin{bmatrix} u_x \\ u_y \end{bmatrix},$$

$$C = \begin{bmatrix} 0 & 1 & 0 & 0 & 0 & -1 & 0 \\ 0 & 0 & 0 & 1 & 0 & 0 & -1 \end{bmatrix}, \quad x = [i_{sx} \ \psi_r \ i_{sy} \ \omega \ m_L \ \psi_r^{ref} \ \omega^{ref}]^T.$$

The MPC controller allows us to limit a control signal as well as a system state. So, during the design process and test, following limitations are specified: for currents in the x and y axes. The cost function used in the work is presented below (22):

$$\min_{\substack{\Delta u_x \\ \Delta u_y}} \left\{ \sum_{k=1}^N \left[q_{11} (\psi_r(k) - \psi_r^{ref}(k))^2 + q_{22} (\omega(k) - \omega^{ref}(k))^2 \right] + \right. \\ \left. + \sum_{p=0}^{N_u-1} \left[r_1 (u_x^{ref}(p)) + r_2 (u_y^{ref}(p)) \right] \right\}, \quad (22)$$

$$|u_{sx}| \leq u_{sx}^{max}, \quad |u_{sy}| \leq u_{sy}^{max}, \quad |i_{sx}| \leq i_{sx}^{max}, \quad |i_{sy}| \leq i_{sy}^{max},$$

where: N is the length of the prediction horizon, N_u is the length of the control horizon, q_{11} , q_{22} represent the weights for outputs, r_1 , r_2 are weights for controls.

The square cost function has better properties in the range of low errors. This form of the cost function was selected for better stabilization of variables near the steady state. During the simulation tests, the weighting factors were selected by a genetic algorithm. Under experimental conditions, the weighting factors have been re-tuned empirically.

4. Results

In the simulation study the properties of the predictive control algorithms with an IM motor drive are investigated. During the design process the mathematical model of drive (21) and cost function (22) is used. The influence of different parameters on regulation properties are tested.

At first, the length of the control horizon is investigated. The following values are selected: one and two samples ahead. The size of the prediction horizon is set to 7. The obtained results are shown in Fig. 2.

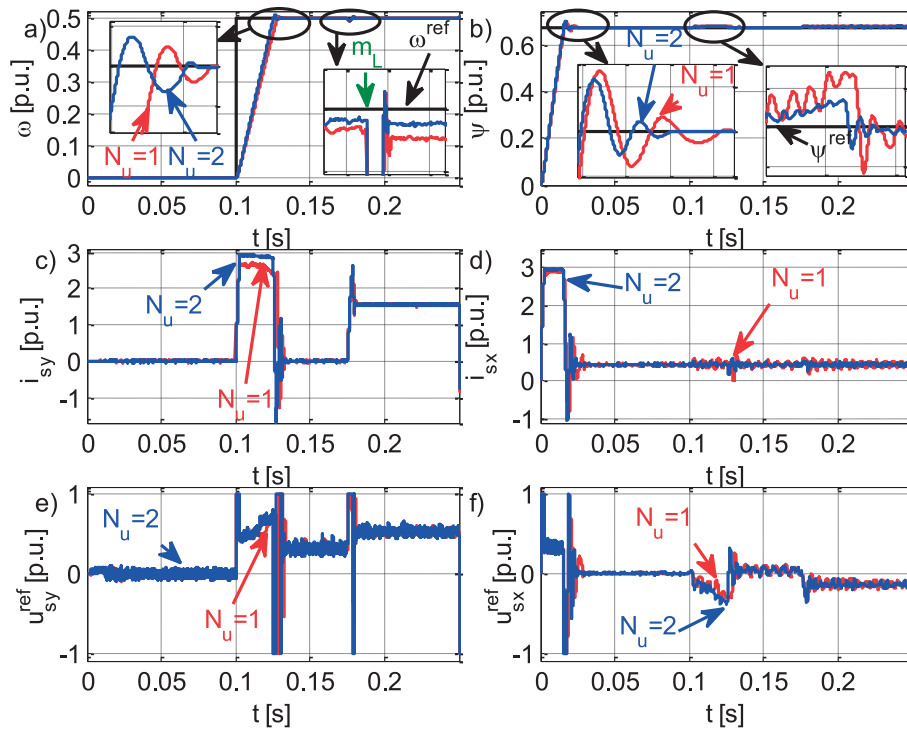


Fig. 2. The transients of system states: speed (a); flux (b); currents (c, d) and voltages (e, f) for different lengths of control horizon

The following remarks can be formulated on the basis of the presented transients. The extension of the control improves the quality of the controlled states significantly. The rising time of the speed is shorter for a longer horizon (Fig. 2(a)). Also, the fluctuations of the speed are smaller. The similar features are visible also in other states (flux, current) of the system. The oscillations in the flux and current are much bigger for the system with a shorter control horizon. Also, the steady-state error is much smaller in all state variables. Additionally, Figs. 2(c), d show the decoupling effect. The component of the current in the x-axis is responsible for generating the flux, while the component in the y-axis is responsible for creating the moment and, consequently, for stabilizing the speed. The relatively different situation exists in the transients of the reference voltage. The limitations of the currents and voltages are kept, which confirms the effectiveness of the MPC algorithm. The system with $N_u = 2$ regulates this signal more dynamically, yet some fluctuations of this signal are evident in steady-state conditions (Figs. 2(e), (f)). During the study the system with the bigger control horizon also has been tested. However, the further extension of the length changes the properties of the system only slightly.

Then the influence of the length of the prediction horizon N is examined. The following parameters are selected in this point: $N_u = 2$, and three different values of $N = 2, 7$ and 14 . The system transients are shown in Fig. 3.

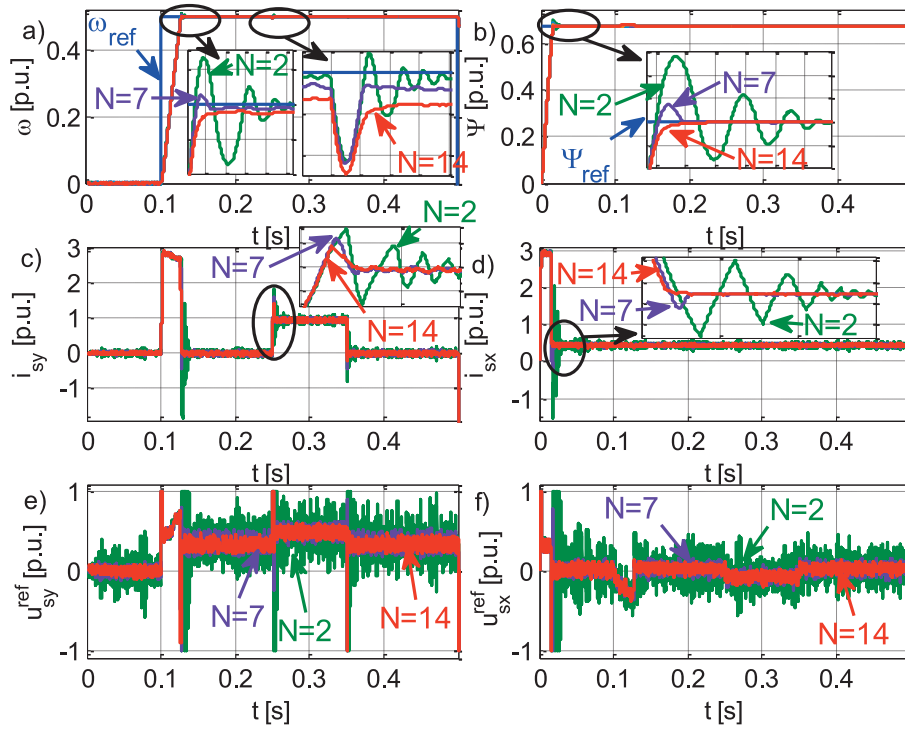


Fig. 3. The transients of system states: speed (a); flux (b); currents (c, d) and voltages (e, f) for different lengths of prediction horizon

From the presented transients the following remarks can be formulated. The length of the predictive horizon does not significantly influence the transients of the speed and flux. They differ from each other relatively slightly. The big difference is noticeable in the currents and reference voltages transients. For the system with a smaller prediction $N = 2$, the big oscillations are evident. The extension of the horizon to $N = 7$ decreases the level of oscillations significantly. The further extension to $N = 14$ does not influence the properties of the system. The oscillation levels remain similar.

Next, the influence of the weights q_{11} and q_{22} , evident in the cost function on the drive dynamics, is tested. The representative transients of the system are shown in Figs. 4(a-f).

As can be concluded from the presented transients, the selection of the weights has a big influence on the system properties. The increase of the value of q_{11} stabilizes the control of the flux better and worsens the speed control slightly. What can be clearly seen, a higher value increases the level of noises in the reference voltage.

Increasing the value of q_{22} improves the quality of the speed control of the system, yet worsens the flux control. It also intensifies the noise level in the reference voltage.

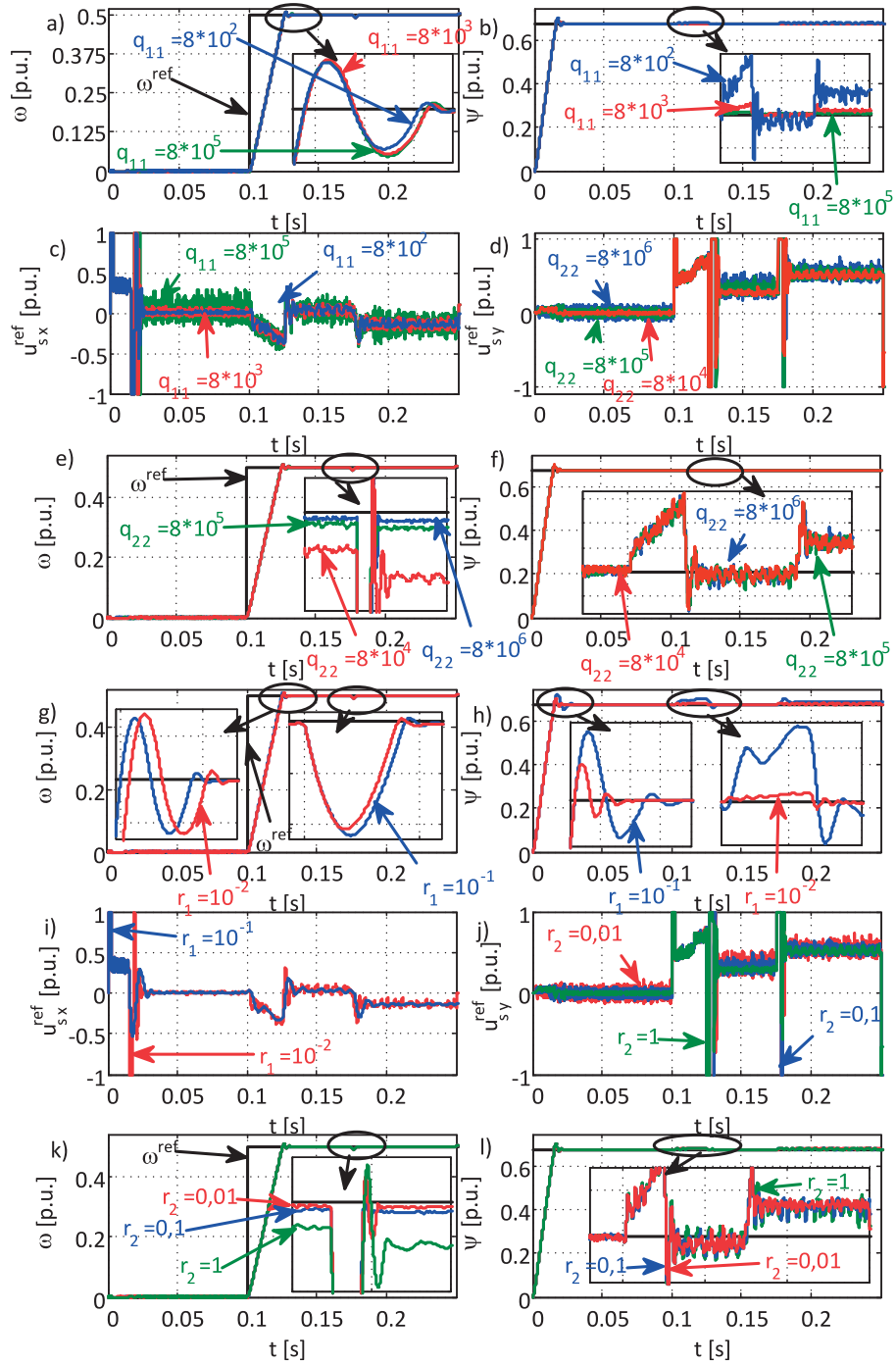


Fig. 4. Transients of system states: speed (a, e, g, k); flux (b, f, h, l) and voltages (c, d, i, j) for different values of the weights: q_{11} (a-c); q_{22} (d-f); r_1 (g-i); r_2 (j-l)

The effect of changing the r_1 and r_2 values is demonstrated in Figs. 4(g–l). The system with a higher value of r_1 possesses a slightly shorter settling time of the speed after changing the reference signal. The bigger difference is visible in the flux transients. This variable oscillates more significantly in this case. The noise levels in the transients of the reference value of the voltages are smaller. The increased value of r_2 causes a bigger steady-state error of the speed and the oscillation level of the flux, yet decreases the noises in the reference voltages.

It can be concluded that controller weights are the main tuning parameters, which differentiate the effect of individual errors on the value of the objective function. With appropriately selected weighting factors, the extension of the prediction horizon allows for an additional improvement in the obtained results. It also allows for earlier detection and reaction to exceeding established constraints.

The influence of the control horizon on the computational complexity of the algorithm is an important task. The number of control regions for $N_u = 1$ is equal to 25 and rises through 209 ($N_u = 2$), 567 ($N_u = 3$) to 851 ($N_u = 4$). The illustration of the numbers of the regions for $N_u = 1$ and $N_u = 2$ are presented in Fig. 5.

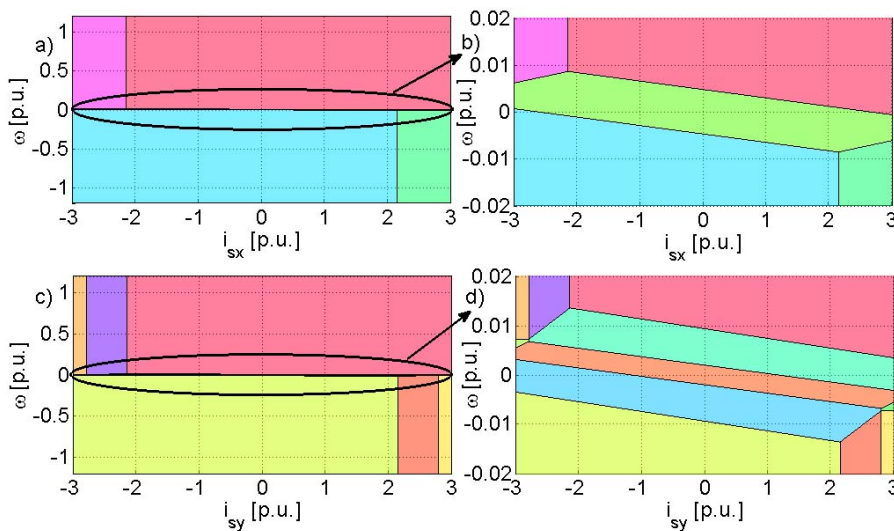


Fig. 5. The hypothetical control surface for $N_u = 1$ (a, b) i $N_u = 2$ (c, d) with $N = 4$

The location of the bigger number of regions around zero stressed the nonlinear relationship of the control signal and speed and currents. The longer control horizon is, the more regions are evident. This is an important task, which limits the extension of the control horizon in practical applications.

Then the system was tested under a variety of experimental tests. The block diagram of the laboratory set-up is presented in Fig. 6.

The experimental set-up is composed of an induction motor with a nominal power of 1.1 kW, driven by a power converter. The motor is coupled to a load machine by a shaft. The speed and position of the motor is measured by incremental encoders (36 000 pulses). The control and

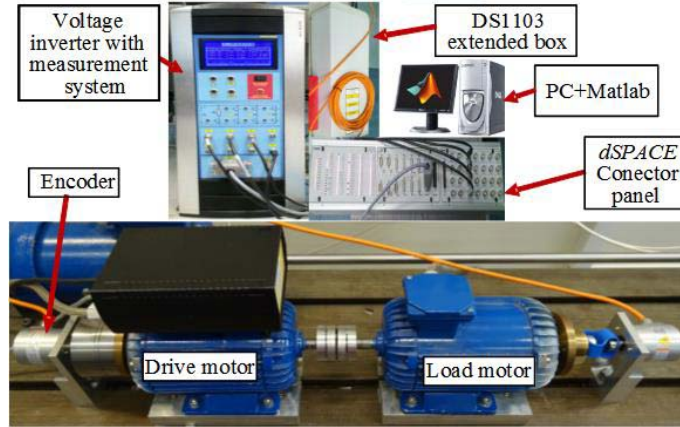


Fig. 6. The block diagram of the laboratory set-up

estimation algorithms have been implemented by a digital signal processor using *dSPACE 1103*. The sampling time of the predictive controller is 0.2 ms. The rotor flux is estimated through a simulator based on the current model [28].

Firstly, the system work under reverse condition and nominal value of the reference speed is tested. The selected transients of the system are shown in Figs. 7(a–c). As can be concluded from the shown transients, the system is working correctly. At the start, there is a short pulse of the current in the x -axis in order to force the nominal value of the flux. Then, at the time $t = 0.1$ s, the reference value of the speed changes and the drive speed follows this signal. During the start-up and the reverse, small errors resulting from the set values of the weights in the cost function are evident in the flux transients.

Secondly, the drive system under a small value of the reference speed is examined. The system transients are shown in Figs. 7(d, f). The flux is kept at its nominal value during the test. From

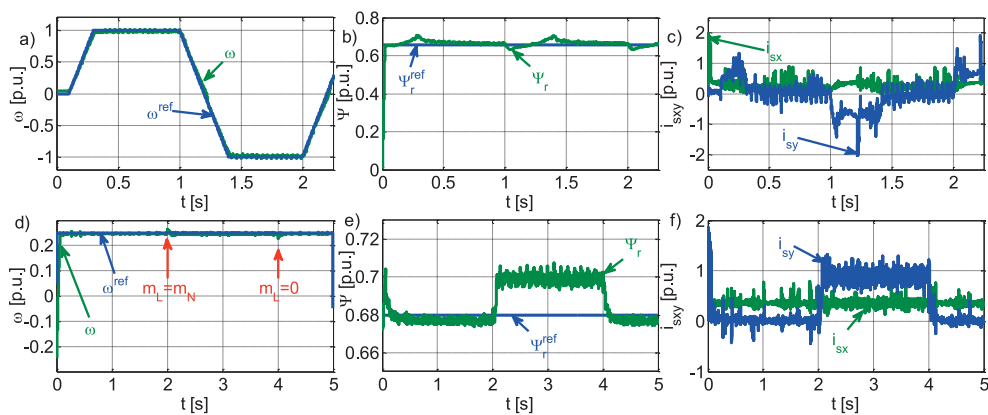


Fig. 7. The transients of selected system states: speed (a, d); flux (b, e) and currents (c, f) for the nominal (a–c) and low (d–f) values of the reference speed

the presented transients, the following remarks can be formulated. The system quickly reaches its nominal value with dynamics limited by the limitation of the current. At the time $t_1 = 2$ and $t_2 = 4$ s the load torque is switched on and off. The controller reacts promptly, only small speed disruptions are visible in the speed transient (Fig. 7(d)). The value of the torque is visible in i_{sy} transients (Fig. 7(f)). In addition, the application of the load torque causes a noticeable decrease in the value of the steady-state error in the flux (Fig. 7(e)).

In the next point, the constraint handling of the MPC controller is investigated. At first, the effect of the changeable limit of the current in the x -axis on the dynamics of the flux is examined. The following values are selected for the test: $i_{sx} = 1, 2, 3$.

The transients of the system are shown in Figs. 8(a, b). As can be expected, the limit of i_{sx} has a significant effect on the dynamics of the flux. The higher is the value of the limit the shorter is the rise time.

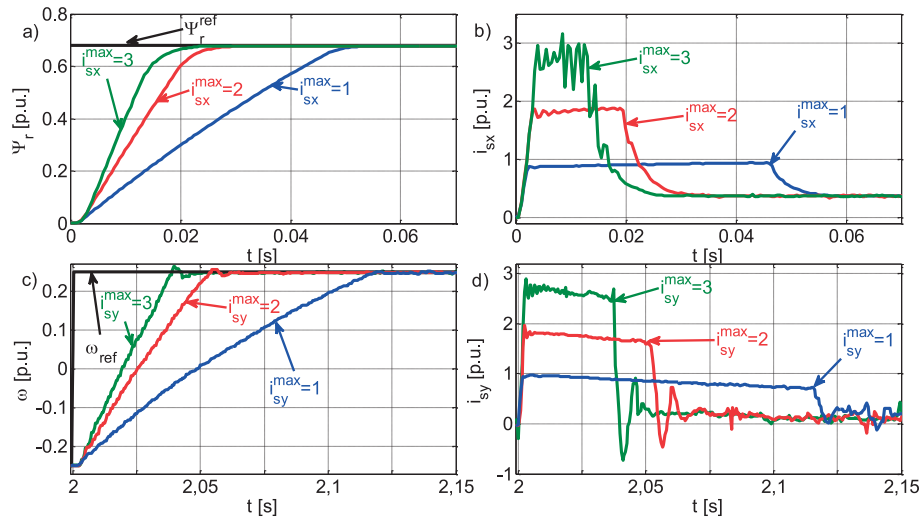


Fig. 8. The transients of system states for different values of the system constraints in currents i_{sx} (a, b) and i_{sy} (c, d)

Then the effect of the limitation of the current in the y -axis is investigated. The limits of the currents are set to $i_{sy} = 1, 2, 3$. The transients of the system are displayed in Figs. 8(c, d).

The tested system is working correctly. Similarly as in the previously considered test, a higher value of the limits causes the reduction of the rise time of the speed. There is no violation of the set limit, which means that the predictive controller is working properly.

5. Conclusion and future study

An MPC control structure of the speed of an induction motor is proposed in the present paper. The control concept refers to the traditional CS-MPC. Contrary to the traditional DFOC control scheme, where four controllers are evident, only one controller is used in the proposed solution.

On the basis of the theoretical considerations and simulation as well as experimental studies, the following concluding remarks can be formulated:

- In order to decrease computational costs, an explicit version of the controller is selected in the paper. It allows the implementation of an MPC algorithm and real-time testing.
- The optimal length of the control horizon should be set during the design process. The controller with one-step N_u works properly, yet some oscillations in the state variables are evident. The extension of this parameter reduces the level of the oscillations but increases the computational demand. So the optimal value of N_u is set to be 2 in the work.
- The length of the prediction horizon plays an even more important role than the previously considered parameter. Its extension reduces the oscillations in the transients, increases computational complexity, yet not as drastically as the control horizon.
- The form of the cost function as well as the used weights have a big influence on the drive performance. Increasing the value of the specific weight boosts the significance of the states connected with this parameter.
- The real-time tests show the proper work of the proposed control algorithm. The system follows the reference signal properly, the disturbances (changes of the load torque) are quickly eliminated from the controlled transients. What is important, the constraints evident in the control algorithm are not validated during the tests.

The future work will be devoted to designing an MPC control structure more robust to parameter variation with respect to the shape of its transients.

References

- [1] Tarczewski T., Skiwski M., Niewiara L.J., Grzesiak L.M., *High-performance PMSM servo-drive with constrained state feedback position controller*, Bulletin of the Polish Academy of Sciences: Technical Sciences, vol. 66, no. 1, pp. 49–58 (2018).
- [2] Tarczewski T., Skiwiński M., Grzesiak L.M., Zieliński M., *Constrained state feedback control of PMSM servo-drive*, Przegląd Elektrotechniczny (in Polish), vol. 94, no. 3, pp. 99–105 (2018).
- [3] Brock S., Pajchrowski T., *Sensorless and energy-efficient PMSM drive for fan application*, Archives of Electrical Engineering, vol. 62, no. 2, pp. 217–225 (2013).
- [4] Ufnalski B., Grzesiak L.M., *Repetitive neurocontroller with disturbance feedforward path active in the pass-to-pass direction for a VSI inverter with an output LC filter*, Bulletin of the Polish Academy of Sciences: Technical Sciences, vol. 64, no. 2, pp. 115–125 (2016).
- [5] Pajchrowski T., Wójcik A., *The problem of rotational speed unevenness in direct drives with permanent magnet synchronous motors*, Przegląd Elektrotechniczny (in Polish), vol. 94, no. 5, pp. 128–132 (2018).
- [6] Brock S., *Application of sliding mode observer for sensorless operation of switched reluctance motors*, Archives of Electrical Engineering, vol. 56, no. 220, pp. 163–172 (2007).
- [7] Rojas Ch.A., Rodriguez J.R., Kouro S., Villarroel F., *Multiobjective Fuzzy-Decision-Making Predictive Torque Control for an Induction Motor Drive*, IEEE Transaction on Power Electronics, vol. 32, no. 8, pp. 6245–6260 (2017).
- [8] Norambuena M., Rodriguez J., Zhang Z., Wang F., Garcia C., Kennel R., *A Very Simple Strategy for High-Quality Performance of AC Machines Using Model Predictive Control*, IEEE Transaction on Power Electronics, vol. 34, no. 1, pp. 794–800 (2019).
- [9] Wang F., Zhang Z., Mei X., Rodriguez J., Kennel R., *Advanced Control Strategies of Induction Machine: Field Oriented Control, Direct Torque Control and Model Predictive Control*, Energies, vol. 11, no. 120, pp. 1–13 (2018).

- [10] Ahmed A.A., Kwon Koh B., Il Lee Y., *A Comparison of Finite Control Set and Continuous Control Set Model Predictive Control Schemes for Speed Control of Induction Motors*, IEEE Transaction on Industrial Informatics, vol. 14, no. 4, pp. 1334–1346 (2018).
- [11] Geyer T., *Algebraic Tuning Guidelines for Model Predictive Torque and Flux Control*, IEEE Transaction on Industry Applications, vol. 54, no. 5, pp. 4464–4475 (2018).
- [12] Siami M., Khaburi D.A., Rodriquez J., *Simplified Finite Control Set-Model Predictive Control for Matrix Converter-Fed PMSM Drives*, IEEE Transaction on Power Electronics, vol. 33, no. 3, pp. 2438–2446 (2018).
- [13] Preindl M., Bolognani S., *Model Predictive Direct Speed Control with Finite Control Set of PMSM Drive Systems*, IEEE Transaction on Power Electronics, vol. 28, no. 2, pp. 1007–1015 (2013).
- [14] Fuentes E.J., Silva C., Quevedo D.E., Silva E.I., *Predictive speed control of a synchronous permanent magnet motor*, Proceedings of IEEE International Conference on Industrial Technology, Gippsland, Australia, pp. 1–6 (2009).
- [15] Belda K., Vosmik D., *Explicit Generalized Predictive Control of Speed and Position of PMSM Drives*, IEEE Transaction on Industrial Electronics, vol. 63, no. 6, pp. 3889–3896 (2016).
- [16] Wróbel K., Serkies P., Szabat K., *Methods of reducing the computational complexity of predictive controller with induction motors*, Proceedings of IEEE 11th International Conference on Power Electronics and Drive Systems, Sydney, Australia, pp. 1060–1063 (2015).
- [17] Fuentes E., Kalise D., Rodrigues J., Kennel R., *Cascade-Free Predictive Speed Control for Electrical Drives*, IEEE Transaction on Industrial Electronics, vol. 61, no. 5, pp. 2176–2184 (2014).
- [18] Serkies P., *Comparison of the dynamic properties of full and cascade speed control based on the FDC method in two-mass drive*, Przegląd Elektrotechniczny (in Polish), vol. 92, no. 5, pp. 60–65 (2016).
- [19] Mayne D., Rawlings J., Rao C., Scokaert P., *Constrained model predictive control: Stability and optimality*, Automatica, vol. 36, no. 6, pp. 789–814 (2000).
- [20] Tondel P., Johansen T., Bemporad A., *An algorithm for multi-parametric quadratic programming and explicit MPC solutions*, Automatica, vol. 39, no. 3, pp. 489–497 (2003).
- [21] Maciejowski J.M., *Predictive Control: with Constraints*, Pearson education (2002).
- [22] Bemporad A., Borrelli F., Morari M., *Model predictive control based on linear programming – The explicit solution*, IEEE Transaction on Automatic Control, vol. 47, no. 12, pp. 1974–1985 (2002).
- [23] Seron M., De Dona J., Goodwin G., *Global analytical model predictive control with input constraints*, Proceedings of 39th IEEE Conference on Decision and Control, Sydney, Australia, pp. 154–159 (2000).
- [24] Hecceg M., Kvasnica M., Jones C., Morari M., *Multi-Parametric Toolbox 3.0*, Proceedings of European Control Conference, Zurich, Switzerland, pp. 502–510 (2013).
- [25] Bemporad A., Morari M., Dua V., Pistikopoulos E., *The explicit linear quadratic regulator for constrained systems*, Automatica, vol. 38, no. 1, pp. 3–20 (2002).
- [26] Bemporad A., Filippi C., *An algorithm for approximate multiparametric convex programming*, Computational optimization and applications, vol. 35, no. 1, pp. 87–108 (2006).
- [27] Tøndel P., Johansen T.A., Bemporad A., *Evaluation of piecewise affine control via binary search tree*, Automatica, vol. 39, no. 5, pp. 945–950 (2003).
- [28] Orłowska-Kowalska T., *Speed sensorless induction motor drives* (in Polish), Wrocław University of Technology Press (2003).